Pamukkale Univ Muh Bilim Derg, 28(1), 72-80, 2022

Pamukkale Üniversitesi Mühendislik Bilimleri Dergisi

Pamukkale University Journal of Engineering Sciences

Vibration analysis of a pre-stressed curved thin plate

Ön gerilmeli eğri ince plakanin titreşim analizi

Can GONENLI[1*], *Hasan OZTURK*[2], *Oguzhan DAS*[3]

[1]Department of Machine Drawing and Construction, Ege Vocational School, Ege University, Izmir, Turkey.
can.gonenli@ege.edu.tr

[2]Department of Mechanical Engineering, Faculty of Engineering, Dokuz Eylul University, Izmir, Turkey.
hasan.ozturk@deu.edu.tr

[3] Department of Motor Vehicles and Transportation Technologies, Bergama Vocational School, Dokuz Eylul University, Izmir, Turkey.
oguzhan.das@deu.edu.tr

Received/Geliş Tarihi: 02.03.2021 Revision/Düzeltme Tarihi: 03.06.2021 doi: 10.5505/pajes.2021.76814
Accepted/Kabul Tarihi: 03.06.2021 Research Article/Araştırma Makalesi

Abstract

In this study, the free vibration analysis of cantilever isotropic thin plate, which is a large deflected, is investigated. The large deflection is obtained by applying an external distributed vertical load on the cantilever plate then fixing from the other end as the deflection is large. The non - linear deflection curve of the largely deflected flexible plate is obtained from the large deflection equation of the beams. The curved thin plate is modeled by using the finite element method considering a four-node quadrilateral flat shell element. The effects of the load parameter on the natural frequency parameters and mode shapes are investigated. The results are given in tables and graphics. In addition, the natural frequency parameters obtained from the present model are compared with those of ANSYS software to verify the reliability and validity of the present model. The load parameter that forms the curved thin plate changes mode shapes of the plate structure.

Keywords: Large deflection, Curved thin plate, Vibration, Pre-stressed, Finite element analysis.

Öz

Bu çalışmada, büyük çökmeli izotropik ince plakanın serbest titreşim analizi incelenmiştir. Büyük çökme, tek tarafı sabitlenmiş plakaya harici bir dağıtılmış dikey yük uygulanarak ve ardından diğer uçtan sabitlenerek elde edilir. Bükülmüş esnek levhanın doğrusal olmayan çökme eğrisi, kirişlerin büyük çökme denkleminden elde edilir. Eğri ince levha, dört düğümlü dörtgen yassı kabuk eleman dikkate alınarak sonlu elemanlar yöntemi kullanılarak modellenmiştir. Yük parametresinin doğal frekans parametreleri ve mod şekilleri üzerindeki etkileri incelenmiştir. Sonuçlar, tablolar ve grafikler halinde verilmiştir. Ek olarak, mevcut modelden elde edilen doğal frekans parametreleri, mevcut modelin güvenilirliğini ve geçerliliğini doğrulamak için ANSYS yazılımı ile karşılaştırılır. Eğri ince levhayı oluşturan yük parametresi, levha yapısının mod şekillerini değiştirir.

Anahtar kelimeler: Büyük çökme, Eğri ince plaka, Titreşim, Öngerilme, Sonlu elemanlar analizi.

1 Introduction

Thin plates have been used in many applications like aircraft, lightweight engineering structures, ship industry, aerospace vehicles, etc. In a few cases, plates can be brought together beneath introductory conditions of displacement without surpassing their flexible limits for different reasons such as optimal design and stronger solidness. Within the previously mentioned ranges, a large deflection issue of plates shows itself and it is vital and essential to decide their static and dynamic characteristics. Therefore, the natural frequency values and mode shapes of the curvilinear plates should be known at the design stage.

In many researches, different mathematical models for curved plates have been considered and investigated for under different boundary and load conditions. Iyengar and Naqvit presented approximate solutions for the non-linear bending of thin rectangular plates considering large deflections for various boundary conditions and numerical results for square plates with uniform lateral load are given [1]. Olson have studied cylindrical shells both for understanding the fundamental shell behaviour and designing shell structures for industrial applications [2]. Petyt and Nath performed the free vibration characteristics of singly curved rectangular plates. The Kantorovich method is employed to diminish the partial differential equations of motion [3]. A new finite difference approach is presented by Bhattacharya for the solution of static and dynamic deflections of plates. The approach can be applied to finite elements with different geometries without any constraints [4]. Wang and El-Sheikh presented a large-deflection mathematical investigation of rectangular plates under uniform lateral loading and the study provides a mathematical procedure that benefits from the software computing capabilities [5]. A complete analysis is provided for plate in-plane vibration with pairs of clamped or free edge conditions imposed on the non-simply supported boundaries and exact solutions are tabulated for a large range of plate aspect ratios by Gorman [6]. Kim et al. performed a series of elastic and elastoplastic large deflection analyses to show how the curvature effects the strength of the plates [7] Senjanovic et al. studied an analytical process for the forecast dynamic characteristics of the thin rectangular plates. Based on finite element analysis, some extra modes were identified, which are defined as the sum and difference of the cross products of beam modes. These natural mode shapes of beam form a complete natural frequency spectrum of a free rectangular plate as a novelty. In their paper, application of the developed procedure was illustrated in the case of a free thin square and rectangular plate [8]. Rawat et al. investigated the thin circular cylindrical shell can vibrate in different modes [9]. The static deflection of

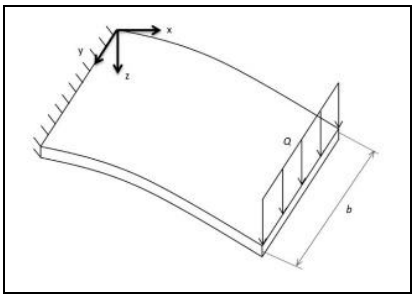
*Corresponding author/Yazışılan Yazar

a thin hyperelastic plate is studied by Amabili et al., and geometrical nonlinearities are modelled according to the Novozhilov nonlinear shell theory [10]. Demir et al. examined the vibration analysis of graphene sheets by modeling as mebrane model, which is thin plates without stiffness against bending and buckling [11]. Qin et al. studied the isogeometric analysis approach for analyse the static deformation, the free vibration and the vibration behaviour of curvilinearly stiffened plates. Also some numerical examples are given to validate the correctness and superiority of their present method [12]. Dogan investigated the effect of curvature ratio on vibration of laminated composite curved shells [13]. Rezaiefar and Galal investigated first three vibration modes for rectangular plates with and without lateral pressure. The vibration frequency increases with increasing the applied lateral pressure [14]. Park et al. studied the structural behaviour of curved plate under axial compression and on the basis of their results, the effects of curvature, initial deflection and boundary conditions are discussed [15]. Eisenberger and Deutsch suggested a new high accuracy mathematical solution that covers all the possible combinations for thin rectangular plate that solve the partial differential equations of motion. Their study also gives examples of their new solution and compared with other approximate solutions [16]. Spagnoli et al. presented an experimental test under static loading on the geometrically non-linear bending of plates. The study shows the critical plate displacement almost independent on the plate size, but linearly depends on the plate thickness [17]. Theoretical and experimental investigation is performed for the Z-shaped folded plates. The nonlinear model of the plate is created depend on the Hamilton standard, von Kármán equations, and the classical plate theory, and ANSYS is employed for the calculation of the vibration mode shape functions [18]. A numerical manifold method, considered to be a generalization of the finite element method, is presented by Guo et al. for vibration analysis of Kirchhoff's plates [19]. Wave based method to predict flexural vibration of thin plate with general elastically restrained edges is subjected by Liu et al [20]. Xue et al. used in-plane preload on nonlinear vibration of cracked rectangular Mindlin plate. The Ritz method is employed to determine the initial in-plane stress resultants [21]. He et al. performed analysis of vibration characteristics of joined cylindrical-spherical shells with using Donnell shell theory to formulate the theoretical model [22].

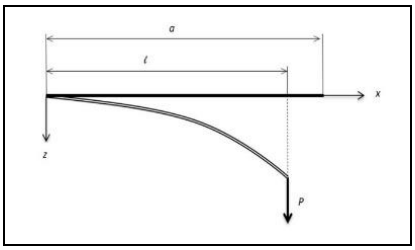
As the curvature of the plate changes, its stiffness also changes, and this situation causes the plate to show different mode shapes. Especially in curvature values where mode shapes change, transition of those mode shapes can cause unpredictable physical damage under operating conditions. This study presents the free vibration examination of pre-stressed isotropic curved thin plate. The consequence of the load parameter on the primary five modes is examined. In order to get pre-stressed isotropic curved thin plate, an external vertical distributed load is applied to the free end of a cantilever plate, and after that the free edge where the load is applied, is fixed. It is ensured that the maximum load is equal to 85% of the yield stress. This value has been previously included in the literature as 75% by Ozturk [23] for the pre-stressed curved beams. In this study, a close value is chosen, provided that it is above 75%. To confirm the efficiency and validity of the theoretical analysis, the natural frequency parameters are compared with ANSYS for same load parameters as used in theoretical analysis. According to the literature review, there are no published studies on this particular topic, and a feasible and reliable method is presented for modeling pre-stressed curved plates.

2 Theoretical analysis

In many such applications, the deformation can be analysed by using a thin plate (or beam) theories [24]. The curvature of the deflection of a thin plate under loading at any point depends on the magnitude of the bending moment under the assumption that the thin plate is linearly elastic. The deflected form of the plate structure is shown in Figure 1.



(a)



(b)

Figure 1. The curvilinear form of the thin plate.
(a): Perspective view. (b): Exact length (a) and projected length (l) of the plate.

Q represents uniformly distributed load. As mentioned above, it is assumed that the deflection of the plate is similar to beam. Ozturk [23] has used beam deflection equation (1) in his study.

$$z(x) = \frac{P}{2EI}\left(-\frac{x^3}{3} + lx^2\right) + \frac{1}{2}\left(\frac{P}{2EI}\right)^3\left(-\frac{x^7}{7} + lx^6 - \frac{12}{5}l^2x^5 + 2l^3x^4\right) + \frac{3}{8}\left(\frac{P}{2EI}\right)^5\left(-\frac{x^{11}}{11} + lx^{10} - \frac{40}{9}l^2x^9 + 10l^3x^8 - \frac{80}{7}l^4x^7 + \frac{16}{3}l^5x^6\right) + \cdots \quad (1)$$

E represents young modulus, P is the force, I denotes the moment of inertia for the plate and l stands for projected length of the plate after the force have been applied. P has been obtained from equation (2).

$$P = Qb \quad (2)$$

Where b represents the width of the plate. The formula given in equation (3) is used to obtain the unknown projected plate length, l.

$$a = \int_0^l \sqrt{1 + \left(\frac{\mathrm{dz}}{\mathrm{dx}}\right)^2}\,\mathrm{dx} \tag{3}$$

By using equation (1), dz/dx and rotation angles are found.

2.1 The finite element model

In order to model curvilinear thin plate, out-of-plane and in-plane vibration theories are combined together and utilized with finite element method. The four-node quadrilateral element considered in this study, has twenty-four degrees of freedom where each node contains six generalized coordinates.

2.1.1 Out-of-plane vibration

The out-of-plane vibration theory is based on the bending vibration of the plate. The finite element model type for the bending vibration is quadrilateral. The strain U_1 and kinetic T_1 energy expressions for a thin plate bending element are:

$$U_1 = \frac{1}{2}\int_A \frac{h^3}{12}\{\chi\}^T[D]\{\chi\}dA$$
$$T_1 = \frac{1}{2}\int_A \rho\, h\dot{w}^2 dA \tag{4}$$

where ρ is the density of the material, h is the thickness, and D is a material matrix and given in equation (5).

$$[D] = \frac{Eh^3}{12(1-\nu^2)}\begin{bmatrix} 1 & \nu & 0 \\ \nu & 1 & 0 \\ 0 & 0 & \dfrac{1-\nu}{2} \end{bmatrix} \tag{5}$$

E and ν represent modulus of elasticity and Poisson Ratio, respectively. The matrix χ given in equation (6) is called the strain-displacement relationship.

$$\{\chi\} = \begin{bmatrix} \partial^2 w/\partial x^2 \\ \partial^2 w/\partial y^2 \\ 2\partial^2 w/\partial x \partial y \end{bmatrix} \tag{6}$$

The four-node quadrilateral finite element, shown in Figure 2 is utilized in this study. Since the out-of-plane theory is considered, three generalized coordinates namely, w, dw/dy, dw/dx are taken into account to represent the flexural displacement and rotation in x and y axis, respectively [25].

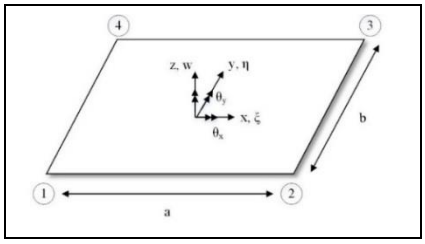


Figure 2. Degrees of freedom for the quadrilateral rectangular plate model for out-of-plane vibration.

The displacement function is given in equation (7).

$$w(x,y) = a_1 + a_2x + a_3y + a_4x^2 + a_5xy + a_6y^2 + a_7x^3 + a_8x^2y + a_9xy^2 + a_{10}y^3 + a_{11}x^3y + a_{12}xy^3 \tag{7}$$

The flexural displacement, w, is written in terms of natural coordinates (ξ,η) instead of Cartesian coordinates (x,y). Hence, dw/dy and dw/dx become:

$$\frac{\partial w}{\partial y} = \frac{2}{b}\frac{\partial w}{\partial \eta}$$
$$\frac{\partial w}{\partial x} = -\frac{2}{a}\frac{\partial w}{\partial \xi} \tag{8}$$

The matrix form of displacement function is:

$$\{\mathrm{w}\} = [A_1]\{\mathrm{q}_1\} \tag{9}$$

Substituting equations (7) and (8) into equation (9) gives the quadratic shape function.

$$N_{1j}^T(\xi,\eta) = \begin{bmatrix} \dfrac{1}{8}(1+\xi_j\xi)(1+\eta_j\eta)(2+\xi_j\xi+\eta_j\eta-\xi^2-\eta^2) \\ \dfrac{b}{2}(1+\xi_j\xi)(\eta_j+\eta)(\eta^2-1) \\ -\dfrac{a}{2}(\xi_j+\xi)(\xi^2-1)(1+\eta_j\eta) \end{bmatrix} \tag{10}$$

(ξ_j,η_j) are the coordinates of node j. The strain displacement matrix B_1 is obtained by equation (11).

$$B_1 = \begin{bmatrix} \dfrac{4}{(a)^2}\dfrac{\partial^2}{\partial\xi^2} \\ \dfrac{4}{(b)^2}\dfrac{\partial^2}{\partial\eta^2} \\ \dfrac{8}{(a)(b)}\dfrac{\partial^2}{\partial\xi\partial\eta} \end{bmatrix} N_1(\xi,\eta) \tag{11}$$

The element stiffness and mass matrix are calculated using equations (12).

$$[K_1] = \int_{-1}^{1}\int_{-1}^{1}[B_1]^T[D][B_1]\mathrm{d}\xi\mathrm{d}\eta$$
$$[M_1] = \rho h\int_{-1}^{1}\int_{-1}^{1}[N_1]^T[N_1]\mathrm{d}\xi\mathrm{d}\eta \tag{12}$$

2.1.2 In-Plane vibration

The finite element model to be used for in-plane vibration must have a total eight corner displacements, including u and v, at each node, and this finite element model is given in Figure 3.

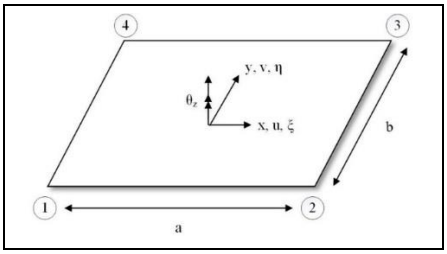


Figure 3. Degrees of freedom for the quadrilateral rectangular plate model for in-plane vibration.

The shape function of in-plate theory is given in equation (13) where ξ_j, η_j are the coordinates of node j [25, 26].

$$N_{2j} = \frac{1}{4}(1+\xi_j\xi)(1+\eta_j\eta) \tag{13}$$

The element displacement components u and v are given in equation (14).

$$\begin{aligned} u &= N_{21}q_{21} + N_{22}q_{23} + N_{23}q_{25} + N_{24}q_{27} \\ v &= N_{21}q_{22} + N_{22}q_{24} + N_{23}q_{26} + N_{24}q_{28} \end{aligned} \tag{14}$$

where q represents the denotes the element displacement vector and can be written in matrix form as,

$$v = N_2 q_2 \tag{15}$$

where,

$$N_2 = \begin{bmatrix} N_{21} & 0 & N_{22} & 0 & N_{23} & 0 & N_{24} & 0 \\ 0 & N_{21} & 0 & N_{22} & 0 & N_{23} & 0 & N_{24} \end{bmatrix} \tag{16}$$

The strain-displacement relations are:

$$\varepsilon = \begin{Bmatrix} \varepsilon_x \\ \varepsilon_y \\ \gamma_{xy} \end{Bmatrix} = \begin{Bmatrix} \dfrac{\partial u}{\partial x} \\ \dfrac{\partial v}{\partial y} \\ \dfrac{\partial u}{\partial y} + \dfrac{\partial v}{\partial x} \end{Bmatrix} \tag{17}$$

Subsequently, it is needed to express the derivatives of the displacement functions, which are in x and y coordinates, in terms of its derivatives in ξ, η coordinates.

$$\begin{Bmatrix} \dfrac{\partial u}{\partial \xi} \\ \dfrac{\partial u}{\partial \eta} \end{Bmatrix} = J \begin{Bmatrix} \dfrac{\partial u}{\partial x} \\ \dfrac{\partial u}{\partial y} \end{Bmatrix}$$

$$\begin{Bmatrix} \dfrac{\partial v}{\partial \xi} \\ \dfrac{\partial v}{\partial \eta} \end{Bmatrix} = J \begin{Bmatrix} \dfrac{\partial v}{\partial x} \\ \dfrac{\partial v}{\partial y} \end{Bmatrix} \tag{18}$$

These equations can be inverted as:

$$\begin{Bmatrix} \dfrac{\partial u}{\partial x} \\ \dfrac{\partial u}{\partial y} \end{Bmatrix} = J^{-1} \begin{Bmatrix} \dfrac{\partial u}{\partial \xi} \\ \dfrac{\partial u}{\partial \eta} \end{Bmatrix}$$

$$\begin{Bmatrix} \dfrac{\partial v}{\partial x} \\ \dfrac{\partial v}{\partial y} \end{Bmatrix} = J^{-1} \begin{Bmatrix} \dfrac{\partial v}{\partial \xi} \\ \dfrac{\partial v}{\partial \eta} \end{Bmatrix} \tag{19}$$

where J is the Jacobian matrix.

$$J = \begin{bmatrix} \dfrac{\partial x}{\partial \xi} & \dfrac{\partial y}{\partial \xi} \\ \dfrac{\partial x}{\partial \eta} & \dfrac{\partial y}{\partial \eta} \end{bmatrix} \tag{20}$$

Equations yield:

$$\varepsilon = A_2 \begin{Bmatrix} \dfrac{\partial u}{\partial \xi} \\ \dfrac{\partial u}{\partial \eta} \\ \dfrac{\partial v}{\partial \xi} \\ \dfrac{\partial v}{\partial \eta} \end{Bmatrix} \tag{21}$$

where A_2 is given by:

$$A_2 = \frac{1}{\det J} \begin{bmatrix} J_{22} & -J_{12} & 0 & 0 \\ 0 & 0 & -J_{21} & J_{11} \\ -J_{21} & J_{11} & J_{22} & -J_{12} \end{bmatrix} \tag{22}$$

From the interpolation equations, it can be written as:

$$\begin{Bmatrix} \dfrac{\partial u}{\partial \xi} \\ \dfrac{\partial u}{\partial \eta} \\ \dfrac{\partial v}{\partial \xi} \\ \dfrac{\partial v}{\partial \eta} \end{Bmatrix} = G q_2 \tag{23}$$

By substituting equation (23) into (21), we obtain,

$$\varepsilon = A_2 G q_2 \tag{24}$$

where,

$$B_2 = A_2 G \tag{25}$$

The stiffness matrix for the quadrilateral finite element is derived from the strain energy via equation (26):

$$U_2 = \int_V \frac{1}{2}\sigma^T \varepsilon dV \tag{26}$$

where σ is given by:

$$\sigma = D B_2 q_2 \tag{27}$$

D is a (3x3) material matrix, The strain energy becomes:

$$U_2 = \frac{1}{2} {q_2}^T \left[h \int_{-1}^{1}\int_{-1}^{1} B_2^T D B_2 \det J \, d\xi d\eta \right] q_2 \tag{28}$$

where K_2 is the stiffness matrix of dimension (8x8).

$$[K_2] = h \int_{-1}^{1}\int_{-1}^{1} B_2^T D B_2 \det J \, d\xi d\eta \tag{29}$$

The element mass matrix M_2 can be found from the kinetic energy.

$$T_1 = \frac{1}{2} {\dot{q}_2}^T \left[\rho h \int_{-1}^{1}\int_{-1}^{1} N_2^T N_2 \det J \, d\xi d\eta \right] \dot{q}_2 \tag{30}$$

The element mass matrix is given in equation (31).

$$[M_2] = \rho h \int_{-1}^{1}\int_{-1}^{1} N_2^T N_2 \det J \, d\xi d\eta \tag{31}$$

2.1.3 Finite element assembly

The final stiffness and the mass matrices are obtained when out-of-plane and in-plane matrices are combined. The relation is given in equation (32).

$$[Out-of-plane,\ K_1\ \&\ M_1]_{12\times12} + [In-plane,\ K_2\ \&\ M_2]_{8\times8} = \begin{bmatrix} 12\times12 & 0 \\ 0 & 8\times8 \end{bmatrix}_{20\times20} \quad (32)$$

This model has six degree-of-freedom (DOF), but the stiffness and mass matrices have (20x20) size matrices. Although these matrices are able to represent the effect of θ_z, last value has to be added formally into those matrices for drilling effect. This relation is given in equation (33).

$$K_e, M_e = \begin{bmatrix} 12\times12 & 0 \\ 0 & 8\times8 \end{bmatrix}_{20\times20} + \theta_z = \begin{bmatrix} 12\times12 & 0 & 0 \\ 0 & 8\times8 & 0 \\ 0 & 0 & 4\times4 \end{bmatrix}_{24\times24} \quad (33)$$

The value of θ_z is taken the absolute value that 1/1000 of the minimum value in (20x20) stiffness and mass matrices by Niyogi [27]. After addition, the finite element model with six DOF is mathematically obtained and is given in Figure 4.

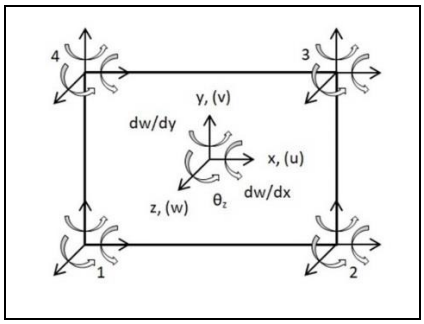
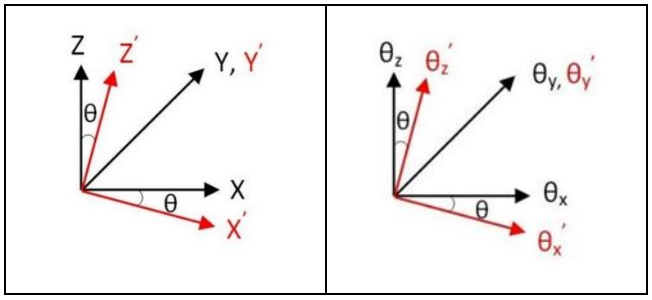


Figure 4. The quadrilateral rectangular straight plate element with six degrees of freedom.

The curvilinear pattern of the plate structure is shaped by end to end addition of rotated strips obtained with finite elements. Hence, it is important to evaluate those rotation angles. These rotation angles are obtained by taking the first derivative of equation (1) with respect to x. Afterward, these values are placed into a transformation matrix which is given in equation (34). It should be noted that the curvilinear plate is modelled by the assembly of rotated element with respect to y-axis by using the transformation matrix. Rotation of the coordinate system is given in Figure 5.



(a) (b)

Figure 5. Rotation of the translation axes. (a): and rotation axes (b).

$$T = \begin{bmatrix} \cos(\theta) & 0 & 0 & 0 & 0 & \sin(\theta) \\ 0 & 1 & 0 & 0 & 0 & 0 \\ 0 & 0 & \cos(\theta) & -\sin(\theta) & 0 & 0 \\ 0 & 0 & \sin(\theta) & \cos(\theta) & 0 & 0 \\ 0 & 0 & 0 & 0 & 1 & 0 \\ -\sin(\theta) & 0 & 0 & 0 & 0 & \cos(\theta) \end{bmatrix} \quad (34)$$

The stiffness and mass matrices can be obtained through the transformation matrix is given in equation (35).

$$K_r = T^T \times K_e \times T \qquad M_r = T^T \times M_e \times T \quad (35)$$

where K_e and M_e represent the stiffness and mass matrices while K_r and M_r are the rotated stiffness and mass matrices of the plate structure.

2.2 Initial stress

The curved plate has a pre-stress because of the distributed load component. After obtaining a curved finite element model, the stress caused by the vertical load on the model is defined. The work done by the in-plane loads is given by equation (36).

$$V = \frac{1}{2}\int_A \left(N_x \left(\frac{dw}{dx}\right)^2 + N_y \left(\frac{dw}{dy}\right)^2 + 2N_{xy}\left(\frac{dw}{dx}\frac{dw}{dy}\right)\right) dxdy \quad (36)$$

The stress effect is called initial stress matrix, and obtained through equation (36) by neglecting N_y and N_{xy}, because the axial load reveals the pre-stress [28].

$$V = \frac{1}{2} N_x \int_A \left(\frac{dw}{dx}\right)^2 dxdy \quad (37)$$

The force N_x is an initial axial force. As can be seen in Figure 6, N_x is obtained from equation (38):

$$N_x = \frac{F_y}{\sin\theta} \quad (38)$$

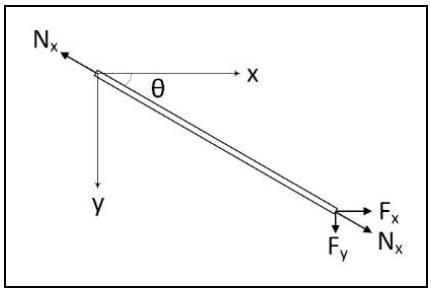


Figure 6. The axial forces in plate element.

where F_y is the total distributed vertical load. Rearranging equation (37) in the matrix form yields equation (39).

$$V = \frac{1}{2} qSq \quad (39)$$

Stiffness matrix K_r, mass matrix M_r and initial stress matrix S_e of each plate element are used to form global stiffness, mass and initial stress matrices. After evaluating the final element

stiffness K_r, mass M_r, and initial stress matrix S_e, global stiffness K, mass M, and initial stress matrices S are obtained. The dynamic response of a plate for the total system can be formulated via equation of motion (40).

$$[M]\{\ddot{q}\} + \left[[K] + [S]\right]\{q\} = 0 \tag{40}$$

Natural frequencies can be obtained via equation (41), where λ denotes natural frequency parameter ω^2.

$$(K + S) - \omega^2 M = 0 \tag{41}$$

3 Results and discussion

The study presents the free vibration of a two edges fixed pre-stressed curved plate. The four-node flat plate element is used to obtain the pre-stressed plate structure, which is large deflected. The plate is discretized into 20x20 finite elements. The properties of the material are given in Table 1.

Table 1. Material specifications and the geometry of the plate.

Symbol	Property	Quantity
E	Modulus of Elasticity	200 GPa
ρ	Mass density	7800 kg/m^3
ν	Poisson's ratio	0.30
a	Length of the plate	1 m
b	Width of the plate	1 m
h	Thickness of the plate	3 mm

The effects of the dimensionless load parameter on the first five natural frequency parameters, λ, are examined. The dimensionless load parameter β is considered between 0 and 1.38. The maximum value of the load parameter equals almost 85% of the yield strength. λ and β are given in equation (42), where A is the cross-section area of the plate, and ω is the natural frequency.

$$\lambda = \omega\sqrt{\frac{\rho A a^4}{EI}} \qquad \beta = \frac{Pa^2}{\nu EI} \tag{42}$$

As the plate is largely deflected, it is fixed from the end on which distributed vertical load is applied. Thus, pre-stressed curved plate is obtained. The free vibration analysis is performed for all considered geometrical forms. The results of the present study are compared with ANSYS to verify the reliability and validity of the present model. A flow chart of the ANSYS software process is given in Figure 7.

Figure 8 shows the deflection of cantilever plate subjected to a distributed vertical load P in terms of the non-dimensional load parameter ranging between 0 and 1.38, $\beta = 0$ represents the flat plate, while $\beta = 1.38$ represents the curved plate in the maximum load condition. Table 2 indicate that the error rates are quite consistent. The error rate does not exceed 6.16% for the first five frequencies, also the error rate remains below 4%, when the maximum load is taken as 60%, (β<1.01), of the yield strength of the material. This, proves the accuracy of the model applied in the present study. The changing of the natural frequency parameters versus the load parameter are given in Figure 9.

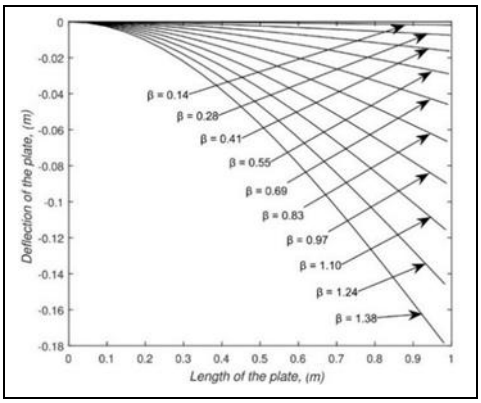


Figure 8. Deflection of a plate under different load parameters.

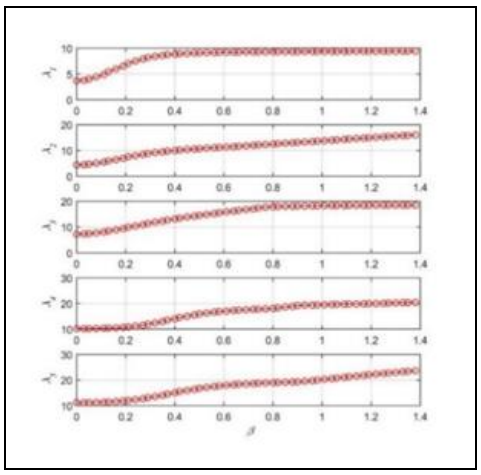


Figure 9. The relationship between the load parameter and the natural frequency parameters.

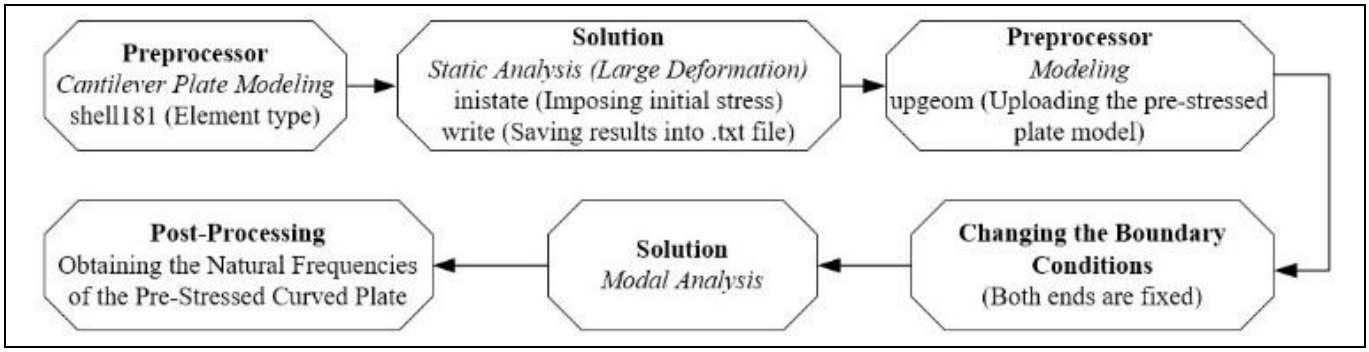


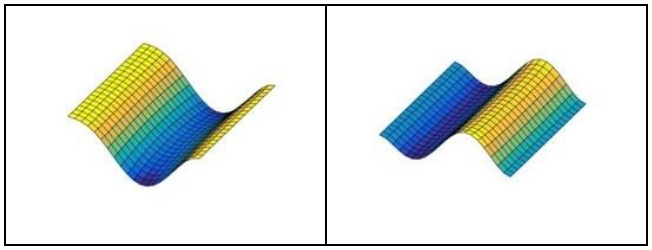
Figure 7. Flowchart of the ANSYS analyzes.

Table 2. Comparison between the present model and ANSYS software results, (λ_1, λ_2, λ_3, λ_4, λ_5)

β	λ_1			λ_2			λ_3			λ_4			λ_5		
	Prsnt	ANSYS	Err (%)	Prsnt	ANSYS	Err (%)	Prsnt	ANSYS	Err (%)	Prsnt	ANSYS	Err (%)	Prsnt	ANSYS	Err (%)
0.00	3.69	3.72	0.73	4.40	4.42	0.52	7.25	7.29	0.51	10.19	10.40	2.00	11.19	11.39	1.72
0.11	4.90	4.85	1.21	5.48	5.45	0.50	8.07	8.04	0.46	10.31	10.51	1.85	11.38	11.56	1.57
0.21	7.05	6.87	2.68	7.54	7.38	2.22	9.94	9.72	2.25	10.88	10.96	0.74	12.07	12.14	0.59
0.32	8.44	8.38	0.72	9.20	9.05	1.68	11.89	11.57	2.76	12.44	12.20	1.98	13.56	13.37	1.41
0.42	8.94	9.01	0.80	10.19	10.09	0.96	13.52	13.16	2.74	14.58	14.16	2.91	15.53	15.16	2.44
0.53	9.13	9.25	1.33	10.89	10.78	1.01	14.91	14.49	2.88	16.28	16.03	1.55	17.17	16.89	1.62
0.64	9.22	9.36	1.49	11.52	11.35	1.50	16.19	15.68	3.26	17.26	17.32	0.36	18.18	18.15	0.21
0.74	9.28	9.42	1.49	12.15	11.88	2.28	17.42	16.77	3.90	17.77	18.06	1.57	18.77	18.91	0.70
0.85	9.32	9.46	1.49	12.80	12.44	2.88	18.06	17.86	1.07	18.61	18.49	0.70	19.15	19.39	1.24
0.96	9.35	9.48	1.42	13.46	12.99	3.65	18.23	18.73	2.69	19.42	18.87	2.93	19.75	19.70	0.27
1.06	9.37	9.50	1.31	14.14	13.55	4.36	18.34	18.89	2.89	19.66	19.82	0.82	20.82	19.93	4.49
1.17	9.39	9.51	1.19	14.81	14.10	5.01	18.42	18.99	3.00	19.89	20.12	1.15	21.83	20.71	5.41
1.27	9.41	9.51	1.05	15.47	14.65	5.53	18.49	19.07	3.06	20.13	20.29	0.80	22.77	21.53	5.77
1.38	9.43	9.52	0.90	16.09	15.19	5.90	18.53	19.12	3.08	20.41	20.47	0.30	23.66	22.29	6.16

As seen from Figure 9 and Table 2, the curve between the natural frequency parameter and the load parameter differs for each natural frequency. The parametric natural frequency values changes in different trends for each load parameter interval. λ_1, λ_2, λ_3 increased apparently in the 0-0.2 range, while λ_4, λ_5 slightly increased. The increase of the first natural frequency parameter between 0.4-1.4, the third natural frequency parameter from β > 0.8, and the fourth natural frequency parameter from β > 1 is negligible. There is no such situation in other natural frequencies. Accordingly, the second natural frequency increases almost linearly when β > 0.2. In the fifth natural frequency, while β = 0.2-0.6, the increase is more apparent than the 0-0.2 range. This increase in the range of 0.6-0.9 started to decrease and became negligible. However, there is a significant increase in the 0.9-1.4 range again. Due to the differences in the mathematical model and analysis method, the error rates are relatively higher in the mode shape change regions and in λ_2 and λ_5, where the curves are in an increasing trend between β = 1.0-1.4. In addition, the effect of the changes in curves on the mode shapes is investigated.

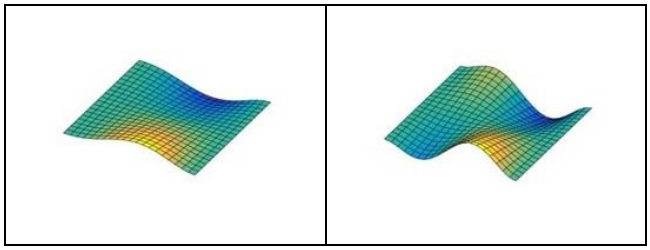
The difference between mode shapes is observed at β = 0.54 for the first natural frequency parameter, as shown in Figure 10.



(a): $0 \le \beta < 0.54$. (b): $0.54 \le \beta \le 1.38$.

Figure 10. Mode shapes of first natural frequency parameter, λ_1, respect to load parameter, β.

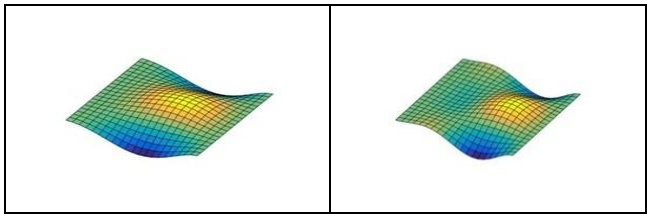
As the load parameter reaches to 0.57, the second mode shape changes. Figure 11 shows the two different mode shapes of the plate structure which are between 0-0.57 and 0.57-1.38.



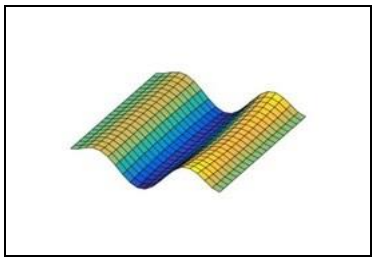
(a): $0 \le \beta < 0.57$. (b): $0.57 \le \beta \le 1.38$.

Figure 11. Mode shapes of second natural frequency parameter, λ_2, respect to load parameter, β.

Three different mode shapes, shown in Figure 12, are observed in the third mode as the load parameter is between 0-0.66, 0.66-1.07, and 1.07-1.38.



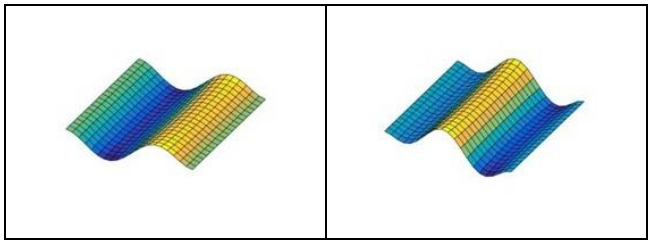
(a): $0 \le \beta < 0.66$. (b): $0.66 \le \beta \le 1.07$.



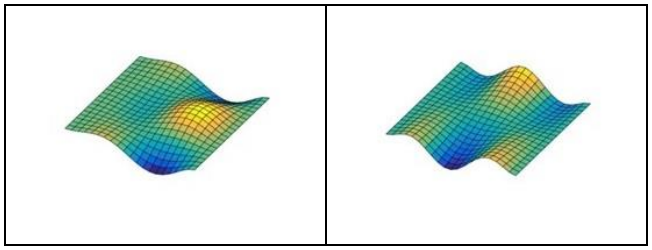
(c): $1.07 \le \beta \le 1.38$.

Figure 12. Mode shapes of third natural frequency parameter, λ_3, respect to load parameter, β.

There are four different mode shapes, shown in Figure 13, in the fourth mode for three different load parameter intervals, 0-0.79, 0.79-1.07, 1.07-1.15, and 1.15-1.38.



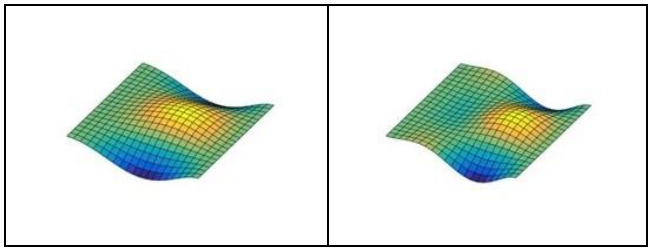
(a): $0 \leq \beta < 0.79$. (b): $0.79 \leq \beta \leq 1.07$.



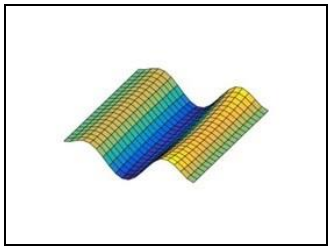
(c): $1.07 \leq \beta < 1.15$. (d): $1.15 \leq \beta \leq 1.38$.

Figure 13. Mode shapes of fourth natural frequency parameter, λ_4, respect to load parameter, β.

The fifth mode comprises three different mode shapes as the load parameter changes. The critical points for those changes are β= 0.79, and β=1.15. The mode shapes that change at these specified load parameter points are given in Figure 14.



(a): $0 \leq \beta < 0.79$. (b): $0.79 \leq \beta \leq 1.15$.



(c): $1.15 \leq \beta < 1.38$.

Figure 14. Mode shapes of fifth natural frequency parameter, λ_5, respect to load parameter, β.

In a nutshell, two different mode shapes in the first and second natural frequencies, three different mode shapes in the third and fifth natural frequencies, and four different mode shapes are observed in the fourth natural frequency. For fundamental frequencies, mode shapes are in a balanced distribution in symmetric geometries. However, the curved plate examined in this study is deflected on the loading edge. This reveals asymmetry. This asymmetry shifts the balanced distribution of the mode shape towards the loading edge and creates new mode shapes. The asymmetry, which remains as the load parameter increases, leads to the emergence of new mode shapes. These new mode shapes cause differences in the behaviour of natural frequency values, as seen from Figure 8.

The first mode, as seen from Figure 9(a), shifted towards the loading edge as the asymmetry increases. Hence, a new mode shape is emerged. This new mode shape emerges where the loading parameter value reaches to 0.54 at which the trend curve of λ_1 changes as seen in Figure 8. The first mode shape Figure 10(a) of the second natural frequency parameter turns into a different mode shape Figure 10(b) by shifting towards the loading edge when the loading parameter value exceeds 0.57. The mode shape Figure 11(a) of the third natural frequency parameter shifts to the new mode shape (Figure 11(b) as the loading parameter value reaches to 0.66. However, as the loading parameter exceeds 1.07, another new mode shape, shown in Figure 11(c), is occurred. Four different modes are observed in the fourth mode as the load parameter reaches to 0.79, 1.07, and 1.15, respectively. The critical loading parameter values are 0.79, 1.07, and 1.15. There are three different mode shapes for the fifth mode, and the critical loading parameter values that changes the mode shapes are 0.79 and 1.15, respectively.

4 Conclusions

This study presents the free vibration analysis of the pre-stressed curved thin plate fixed from both ends. To obtain the curved plate structure, first, it is fixed from one end. Then a distributed vertical load is applied on the free edge of the structure. The plate is deflected by applying such a load. Finally, the deflected structure is fixed from its free end. The curvilinear geometry of the plate structure is modelled by rotating flat plate element. The maximum vertical distributed load is taken a value that brings the plate up to 85% of its yield stress value, due to the operating conditions. All results obtained from the present model are in a close agreement with ANSYS software results. It is essential to understand the dynamic properties of pre-stressed plate structures under several loading conditions. This study reveals the change of dynamic behaviour of the pre-stressed curved plate structure as the parametric load, which is the function of the distributed vertical load, increases. Based on all results presented within this study, the conclusions are as follows:

Knowing dynamic behaviours under operating conditions is important in terms of predicting the damages that may occur in the structure due to concepts such as resonance and stability. In this study, the dynamic behaviour of the pre-stressed curved thin plate structure is examined.

- In all loading cases up to 85% of the yield stress value of the plate, the present model represents the pre-stressed curved thin plate model accurately,
- The error rates are acceptable and partially better for the first, third and fourth natural frequency parameters, where they are mostly tended to remain stable than the second and fifth natural frequency parameters,
- Various curvature values of the structure occurs as the applied load increases. This causes mode shape differences at the same modes,
- The asymmetry of the curved plate shifts the pattern of the mode shape to the edge on which the loading is present.
- As the asymmetry of the curved plate becomes apparent, different mode shapes emerge,
- In the light of the results, the method used in this study provides a simple and fast alternative way for modelling and multiple analysis of curved plates,

- In future studies, different and complex plate structures can be modeled, and static and dynamic analysis of pre-stressed curved plates can be performed by considering the presented method in this study.

5 Author contribution statements

In the present work, Can GONENLI conceived the presented idea, performed analyses, and literature review; Hasan OZTURK supervised the work and evaluated the results; Oguzhan DAS verified the computations and contributed to spelling and checking the article in terms of content. All authors discussed the results and contributed to the final manuscript.

6 Ethics committee approval and conflict of interest statement

There is no need to obtain an ethics committee approval for the presented article. There is no conflict of interest with any person/institution for the presented article.

7 References

[1] Iyengar KR, Naqvi M. "Large deflections of rectangular plates". *International Journal of Non-Linear Mechanics*, 1(2), 109-122, 1966.

[2] Olson MD, Lindberg GM. "Vibration analysis of cantilevered curved plates using a new cylindrical shell finite element". *Proceedings of the Conference on Matrix Methods in Structural Mechanics (2nd)*, Ottawa, Canada, 15-17 October 1968.

[3] Petyt M, Nath JD. "Vibration analysis of singly curved rectangular plates". *Journal of Sound and Vibration*, 13(4), 485-497, 1970.

[4] Bhattacharya M. "Static and dynamic deflections of plates of arbitrary geometry by a new finite difference approach". *Journal of Sound and Vibration*, 107(3), 507-521, 1986.

[5] Wang D, El-Sheikh A. "Large-deflection mathematical analysis of rectangular plates". *Journal of Engineering Mechanics*, 131(8), 809-821, 2005.

[6] Gorman D. "Exact solutions for the free in-plane vibration of rectangular plates with two opposite edges simply supported". *Journal of Sound and Vibration*, 294, 131-161, 2006.

[7] Kim J, Park J, Lee K, Kim JH, Kim MH, Lee JM. "Computational analysis and design formula development for the design of curved plates for ships and offshore structures". *Structural Engineering and Mechanics*, 49(6), 705-726, 2014.

[8] Senjanovic I, Tomic M, Vladimir N, Hadzic N. "An approximate analytical procedure for natural vibration analysis of free rectangular plates". *Thin-Walled Structures*, 95, 101-114, 2015.

[9] Rawat A, Matsagar V, Nagpal A. "Finite element analysis of thin circular cylindrical shells". *Proceedings of the Indian National Science Academy*, 82(2), 349-355, 2016.

[10] Amabili M, Balasubramanian P, Breslavsky I, Giovanni F, Garziera R, Riabova K. "Experimental and numerical study on vibrations and static deflection of a thin hyperelastic plate". *Journal of Sound and Vibration*, 385, 81-92, 2016.

[11] Demir C, Mercan K, Ersoy H, Civalek O. "Vibration analysis of graphene sheets using membrane model". *Pamukkale University Journal of Engineering Sciences*, 23(6), 652-658, 2017.

[12] Qin X, Dong C, Wang F, Qu XY. "Static and dynamic analyses of isogeometric curvilinearly stiffened plates". *Applied Mathematical Modelling*, 45, 336-364, 2017.

[13] Dogan A. "The effect of curvature on transient analysis of laminated composite cylindrical shells on elastic foundation". *Pamukkale University Journal of Engineering Sciences*, 24(6), 960-966, 2018.

[14] Rezaiefar A, Galal K. "Free vibration of thin rectangular steel plates with geometrically-nonlinear load-displacement behavior". *Thin-Walled Structures*, 129, 381-390, 2018.

[15] Park J, Paik J, Seo J. "Numerical investigation and development of design formula for cylindrically curved plates on ships and offshore structures". *Thin-Walled Structures*, 132, 93-110, 2018.

[16] Eisenberger M, Deutsch A. "Solution of thin rectangular plate vibrations for all combinations of boundary conditions". *Journal of Sound and Vibration*, 452, 1-12, 2019.

[17] Spagnoli A, Brighenti R, Biancopsino M, Rossi M, Roncella R. "Geometrically non-linear bending of plates: Implications in curved building facades". *Construction and Building Materials*, 214, 698-708, 2019.

[18] Guo X, Zhang Y, Zhang W, Sun L. "Theoretical and experimental investigation on the nonlinear vibration behavior of z-shaped folded plates with inner resonance". *Engineering Structures*, 182, 123-140, 2019.

[19] Guo H, Zheng H, Zhuang X. "Numerical manifold method for vibration analysis of Kirchhoff's plates of arbitrary geometry". *Applied Mathematical Modelling*, 66, 695-727, 2019.

[20] Liu L, Corradi R, Ripamonti F, Rao Z. "Wave based method for flexural vibration of thin plate with general elastically restrained edges". *Journal of Sound and Vibration*, 483, 1-24, 2020.

[21] Xue J, Wang Y, Chen L. "Nonlinear vibration of cracked rectangular Mindlin plate with in-plane preload". *Journal of Sound and Vibration*, 481, 1-22, 2020.

[22] He Q, Dai HL, Gui QF, Li JJ. "Analysis of vibration characteristics of joined cylindrical-spherical shells". *Engineering Structures*, 218, 1-14, 2020.

[23] Ozturk H. "In-plane free vibration of a pre-stressed curved beam obtained from a large deflected cantilever beam". *Finite Elements in Analysis and Design*, 47, 229-236, 2011.

[24] Jairazbhoy V, Petukhov P, Qu J. "Large deflection of thin plates in convex or concave cylindrical bending". *Journal of Engineering Mechanics*, 138(2), 230-234, 2012.

[25] Petyt M. *Introduction to Finite Element Vibration Analysis*. 2nd ed. New York, USA, Cambridge University Press, 2010.

[26] Chandrupatla T, Belegundu A. *Introduction to Finite Elements in Engineering*. 3rd ed. New Jersey, USA, Prentice Hall, 2002.

[27] Niyogi A, Laha M, Sinha P. "Finite element vibration analysis of laminated composite folded plate structures". *Shock and Vibration*, 6(5-6), 273-283, 1999.

[28] Yang T. "Matrix displacement solution to elastica problems of beams and frames". *International Journal of Solids and Structures*, 9(7), 829-842, 1973.